Electronic Supplementary Information for

Tailoring Biomimetic Polymer Networks towards an Unprecedented Combination of Versatile Mechanical Characteristics

Eun Jung Cha,† Dong Soo Lee,† Hyohye Kim, Yun Ho Kim, Byoung Gak Kim, Youngjae Yoo, Yong Seok Kim, and Dong-Gyun Kim*

Advanced Materials Division, Korea Research Institute of Chemical Technology, 141 Gajeong-ro, Yuseong-gu, Daejeon 34114, Republic of Korea.

* Corresponding author: D.-G. Kim (E–mail: dgkim@krict.re.kr)

† These authors contributed equally to this work.

Table of Contents

Experimental Section

Materials

1,1'-Thiocarbonyldiimidazole (TCDI, >95%, Tokyo Chemical Industry), 1,1'-carbonyldiimidazole (CDI, >97%, Tokyo Chemical Industry), 1,2-bis(2-aminoethoxy)ethane (EGDA, 98%, Sigma-Aldrich), 1,8-diaminooctane (ODA, 98%, Sigma-Aldrich), triglycidyl isocyanurate (TGIC, Sigma-Aldrich), trimethylolpropane triglycidyl ether (TMPTGE, Sigma-Aldrich), *N*,*N*-dimethylformamide (DMF, anhydrous, 99.8%, Sigma-Aldrich), and *N*-methyl-2-pyrrolidone (NMP, anhydrous, 99.5%, Sigma-Aldrich) were used as received. All other reagents and solvents were used as received from standard vendors.

Synthesis of Poly(ether-thiourea) with Triethylene Glycol as a Spacer (TUEG)

Poly(ether-thiourea)s with triethylene glycol as a spacer are designated as TUEG#, where # indicates the average degree of polymerization (DP) as estimated by ^{1}H NMR end group analysis. The following procedure was used for the synthesis of TUEG7 in Table S1 (presented later in this Supporting Information). Preparation procedure was conducted under a nitrogen atmosphere in a glove box (<0.1 ppm of H_2O and O_2). EGDA (5.0 g, 34 mmol) and DMF (15 mL) were placed into a 100 mL round-bottomed flask with a magnetic stirring bar, and TCDI (5.0 g, 28 mmol) was added into the flask under stirring. The reaction flask sealed with stopper was transferred to a thermostatted oil bath at 25 °C outside the glove box. After stirred for 24 h, the solution was diluted by chloroform (15 mL) and precipitated into an excess of ether (800 mL). The dissolution-precipitation procedure was repeated three times. The resulting precipitate was subsequently dried under vacuum at 120 °C overnight, yielding a yellowish solid (4.7 g, 88%). TUEG18 and TUEG34 were prepared using the same procedure, varying the ratio of the TCDI and EGDA monomer charges; molar feed ratios ([TCDI]:[EGDA]) of 1:1.1 and 1:1.05 were used for TUEG18 and TUEG34, respectively. ^{1}H NMR of TUEG34 (400 MHz, DMSO-*d*$_6$, δ/ppm, tetramethylsilane (TMS) ref) (Fig. S2a): 7.54 (br, C(S)N*H*), 3.60-3.20 (br, C*H*$_2$O, C(S)NHC*H*$_2$), 2.68 (t, C*H*$_2$NH$_2$). The DP was determined from the intensity ratio between the peaks at 7.54 (br, C(S)N*H*) and 2.68 (t, C*H*$_2$NH$_2$) ppm.

Synthesis of Poly(alkylene-thiourea) with Octamethylene as a Spacer (TUC)

Poly(alkylene-thiourea) with octamethylene as a spacer is designated as TUC#, where # indicates the average DP as estimated by ^{1}H NMR end group analysis. The following procedure was used for the synthesis of TUC46 in Table S1. Preparation procedure was conducted under a nitrogen atmosphere in a glove box (<0.1 ppm of H_2O and O_2). ODA (4.2 g, 29 mmol) and DMF (15 mL) were placed into a 100 mL round-bottomed flask with a magnetic stirring bar, and TCDI (5.0 g, 28 mmol) was added into the flask

under stirring. The reaction flask sealed with stopper was transferred to a thermostatted oil bath at 60 °C outside the glove box. After stirred for 24 h, the solution was cooled to room temperature and precipitated into an excess of ether (800 mL). The resulting precipitate was filtrated, washed with an excess amount of chloroform and methanol, and subsequently dried under vacuum at 120 °C overnight, yielding a yellowish solid (4.7g, 90%). ^{1}H NMR of TUC46 (400 MHz, DMSO-d_6, δ/ppm, TMS ref) (Fig. S2b): 7.31 (br, C(S)NH), 3.50-3.10 (br, C(S)NHCH_2), 2.76 (t, CH_2NH$_2$), 1.45 (br, C(S)NHCH$_2$CH_2, CH_2CH$_2$NH$_2$), 1.26 (br, CH$_2$(CH_2)$_4$CH$_2$). The DP was determined from the intensity ratio between the peaks at 7.31 (br, C(S)NH) and 2.76 (t, CH_2NH$_2$) ppm.

Synthesis of Poly(ether-urea) with Triethylene Glycol as a Spacer (UEG)

Poly(ether-urea) with triethylene glycol as a spacer is designated as UEG#, where # indicates the average DP as estimated by ^{1}H NMR end group analysis. The following procedure was used for the synthesis of UEG107 in Table S1. Preparation procedure was conducted under a nitrogen atmosphere in a glove box (<0.1 ppm of H$_2$O and O$_2$). EGDA (4.8 g, 32 mmol) and NMP (15 mL) were placed into a 100 mL round-bottomed flask with a magnetic stirring bar, and CDI (5.0 g, 31 mmol) was added into the flask under stirring. The reaction flask sealed with stopper was transferred to a thermostatted oil bath at 90 °C outside the glove box. After stirred for 24 h, the solution was cooled to room temperature and precipitated into an excess of acetone (800 mL). The resulting precipitate was filtrated, washed with an excess amount of methanol, and subsequently dried under vacuum at 140 °C overnight, yielding a yellowish solid (4.5g, 93%). ^{1}H NMR of UEG107 (400 MHz, D$_2$O, δ/ppm) (Fig. S2c): 3.67 (br, OCH_2CH_2O), 3.58 (t, C(O)NHCH$_2$CH_2, CH_2CH$_2$NH$_2$), 3.31 (t, C(O)NHCH_2), 2.94 (t, CH_2NH$_2$). The DP was determined from the intensity ratio between the peaks at 3.31 (t, C(O)NHCH_2) and 2.94 (t, CH_2NH$_2$) ppm.

Preparation of Cross-linked TUEG-TGIC Films (BMPNs)

Cross-linked TUEG-TGIC films are designated as BMPN#, where # indicates the weight percentage (wt %) of TGIC in the film. The following procedure was applied for the preparation of BMPN8. TUEG18 (0.65 g, 0.36 mmol) and TGIC (0.055 g, 0.54 mmol) in DMF (3.5 mL) were cast onto a Teflon plate (7 × 3 cm^2), followed by drying on a hot plate at 50 °C overnight. After subsequently dried at 80 °C under vacuum for 1 h, the resultant film on a Teflon plate was cured at 120 °C for 2 h and postcured at 150 °C for 2 h under vacuum. BMPN4 and BMPN17 were prepared using the same procedure, except the use of TUEG34 and TUEG7 for BMPN4 and BMPN17, respectively. The molar feed ratio of amine end group of TUEG to epoxy group of TGIC ([amine] : [epoxy]) was fixed at 1:1.5 for all the films; this is for the complete reaction of the primary amine and epoxy groups without any unreacted, residual primary amine end-groups or epoxy functional groups.[S1] Cross-linked TUEG-TMPTGE film (BMPN17 with TMPTGE crosslinker; 17 wt % of TMPTGE in the film) was also prepared for comparison purposes using

the same procedure. The thickness of the BMPNs was in the range of 350–400 μm. All the films were additionally dried at 50 °C under vacuum for 24 h before analyses.

Instrumentation and Characterization Techniques

^{1}H NMR and ^{13}C NMR spectra of TUEGs, TUC46, and UEG107 were recorded on a Bruker Ascend 400 MHz using DMSO-d_6 (for TUEGs and TUC46) and D_2O (for UEG107) as solvents. Number-average molecular weights (M_n) and molecular weight dispersities ($Đ$) of TUEGs and TUC46 were determined by gel permeation chromatography (GPC) in DMF (with 0.01M LiBr), using a YL9112 Isocratic pump, a 30 cm Shodex KF-805L column, and a YL9170 differential refractive index (RI) detector operating at 40 °C. The GPC-RI elution time data were calibrated with narrow-distribution polystyrene standards. M_n and $Đ$ of UEG107 were analyzed by GPC in H_2O (pH = 7, with 0.2M $NaNO_3$ and 0.01M NaH_2PO_4), equiped a Waters Alliance e2695 separation module in series with a Waters 2414 RI detector operating at 35 °C. The system was calibrated using narrow-distribution polyethylene glycol standards. Furier transform infrared (FT-IR) spectra were recorded on an Agilent 4100 Exoscan FTIR spectrometer using attenuated total reflectance (ATR) equipment. Single wavelength laser source utilized for light-to-heat conversion test was HB-808-1000 laser (808 nm, 1000 mW, spot diameter = 2.5 mm, High Lasers). Increase in temperature upon NIR irradiation on BMPN8 film was observed by infrared (IR) camera (T300, FLIR). Solvent extraction experiment was performed by placing a small piece (ca. 20 mg) of BMPN films into a 20 mL vial filled with DMF. After stored in an oven at 25 °C for 48 h, the film was recovered and dried at 120 °C under vacuum for 18 h. Gel fraction (f_g) was calculated as

$$f_g = W_a / W_d \qquad (1)$$

where W_d and W_a are the weights of dried film before and after the DMF solvent extraction. The thermal stability of BMPNs was investigated by thermal gravimetric analysis (TGA) using a TA Instruments TGA Q5000 under a nitrogen atmosphere. The samples were first heated to 130 °C and maintained at 130 °C for 10 min in order to evaporate residual water, and then heated to 650 °C at a heating rate of 10 °C min^{-1}. Differential scanning calorimetry (DSC) was run using a TA Instruments DSC Q1000 under a nitrogen atmosphere. Samples with a typical mass of 5–10 mg were encapsulated in sealed aluminum pans. They were first heated from 25 °C to 200 °C and then cooled down to –50 °C, which were followed by second heating at a constant rate of 10 °C min^{-1} (5 °C min^{-1} for UEG107). Surface morphology of BMPN8 was characterized using atomic force microscopy (AFM, Nanoscope IV, Digital Instrument) in tapping mode (TM), using force modulation mode probes (force constant = 42 N m^{-1}, resonance frequency = 320 kHz) purchased from NanoWorld. Wide-angle X-ray scattering (WAXS) was performed using a Rigaku SmartLab. The applied voltage and current were 45 kV and 200 mA, respectively. The samples were mounted on aluminum holder and scanned from 5° to 40°. Small-angle X-ray scattering (SAXS) patterns were acquired using a Rigaku SmartLab with X-rays having 1.5418 Å of

wavelength and generated at 45 kV and 200 mA. SAXS measurements were carried out at ambient conditions, and instrumental background was corrected by subtracting scattering intensity measured from the empty cell.

Mechanical Characterization of TUEG, TUC, UEG, and BMPNs

Dynamic mechanical analysis (DMA) was performed on a TA Instruments DMA Q800 with attached cryo accessory using rectangular-shaped BMPN films (ca. 30 mm (L) × 5 mm (W) × 0.35 mm (T)). DMA was conducted in the film tension mode with a 2.5 Hz frequency, 0.1% strain, and 0.1 N axial force. The specimens were first cooled down from room temperature to −50 °C and then heated to 95 °C at a constant rate of 5 °C min⁻¹ in a nitrogen atmosphere. Cross-linking density (v_e) of BMPNs was calculated as

$$v_e = E' / 3RT \tag{2}$$

where E', R, and T are the storage modulus, universal gas constant, and absolute temperature in the rubbery region (ca. 353.15 K), respectively. Quantitative shape memory behavior of BMPN8 film (ca. 30 mm (L) × 5 mm (W) × 0.35 mm (T)) was evaluated by the same TA Instruments DMA Q800 with attached cryo accessory under controlled force mode. The sample was first heated from 25 °C to 50 °C at a constant rate of 5 °C min⁻¹ and maintained at 50 °C for 10 min. The sampe was subsequently stretched under a load of 0.2 Mpa for 5 min, followed by cooling to 0 °C at a rate of 5 °C min⁻¹ under the load (sample length = ε_{load}) to fix temporary shape. After unloading, the sample maintained the temporary shape with length of ε_{unload}. Shape recovery process was then triggered by heating the sample back to 50 °C at a rate of 5 °C min⁻¹, which decreased the sample length to ε_{rec}. Consecutive shape memory cycles were investigated by repeating the above shape memory cycle. Shape fixity ratio (R_f) and shape recovery ratio (R_r) were calculated as

$$R_f = (\varepsilon_{unload} / \varepsilon_{load}) \times 100\% \tag{3}$$

$$R_r = [(\varepsilon_{unload} - \varepsilon_{rec}) / \varepsilon_{unload}] \times 100\% \tag{4}$$

Shape memory behaviors of BMPNs were also confirmed qualitatively; the BMPN films were deformed to a temporary shape at 50 °C in an oven and then cooled to 0 °C in a refrigerator to fix the temporary shape, which was subsequently placed in an oven at 50 °C or subjected to NIR irradiation to recover the permanent shape. Solvent-induced shape recovery of BMPN8 was tested by placing the deformed BMPN8 into various solvents at 25 °C. Uniaxial tensile testing was carried out on an Instron LR5K universal testing machine (UTM, Lloyd Instruments) at a strain rate of 0.013 s⁻¹ (20 mm min⁻¹) unless otherwise noted. Rectangular shaped tensile bars (ca. 60 mm (L) × 5 mm (W) × 0.4 mm (T), gauge length = 25 mm) were stamped out from the films using a cutting die. At least three different samples

were prepared from each film and tested in the UTM. TUEG34, TUC46, and UEG107 films for tensile testing were prepared by placing the polymers into a Teflon mold (65 mm (L) × 40 mm (W) × 0.5 mm (T)) sandwiched with a Teflon film and pressing (2 MPa) at 120 °C for 30 min. Cyclic tensile testing was performed on the same UTM using the rectangular shaped BMPN films at a strain rate of 0.0067 s^{-1} (10 mm min^{-1}). The samples in between cyclic tests were stored in a vacuum oven at 25 °C to avoid possible water uptake from the air during the recovery time. All the tensile tests were performed at room temperature and humidity (26±1 °C, RH 45±8% in air), unless otherwise noted. Uniaxial tensile testing at different temperatures other than room temperature was also conducted using an Withlab WL2100 UTM with temperature controlled chamber in air at a strain rate of 0.013 s^{-1}.

Synthesis of TUEGs, TUC, and UEG
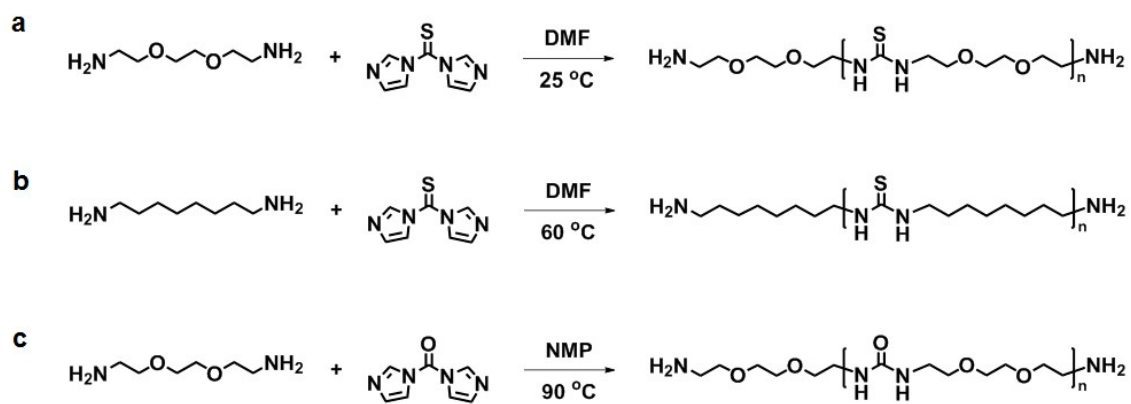
Fig. S1 Synthesis of (a) TUEG, (b) TUC, and (c) UEG.
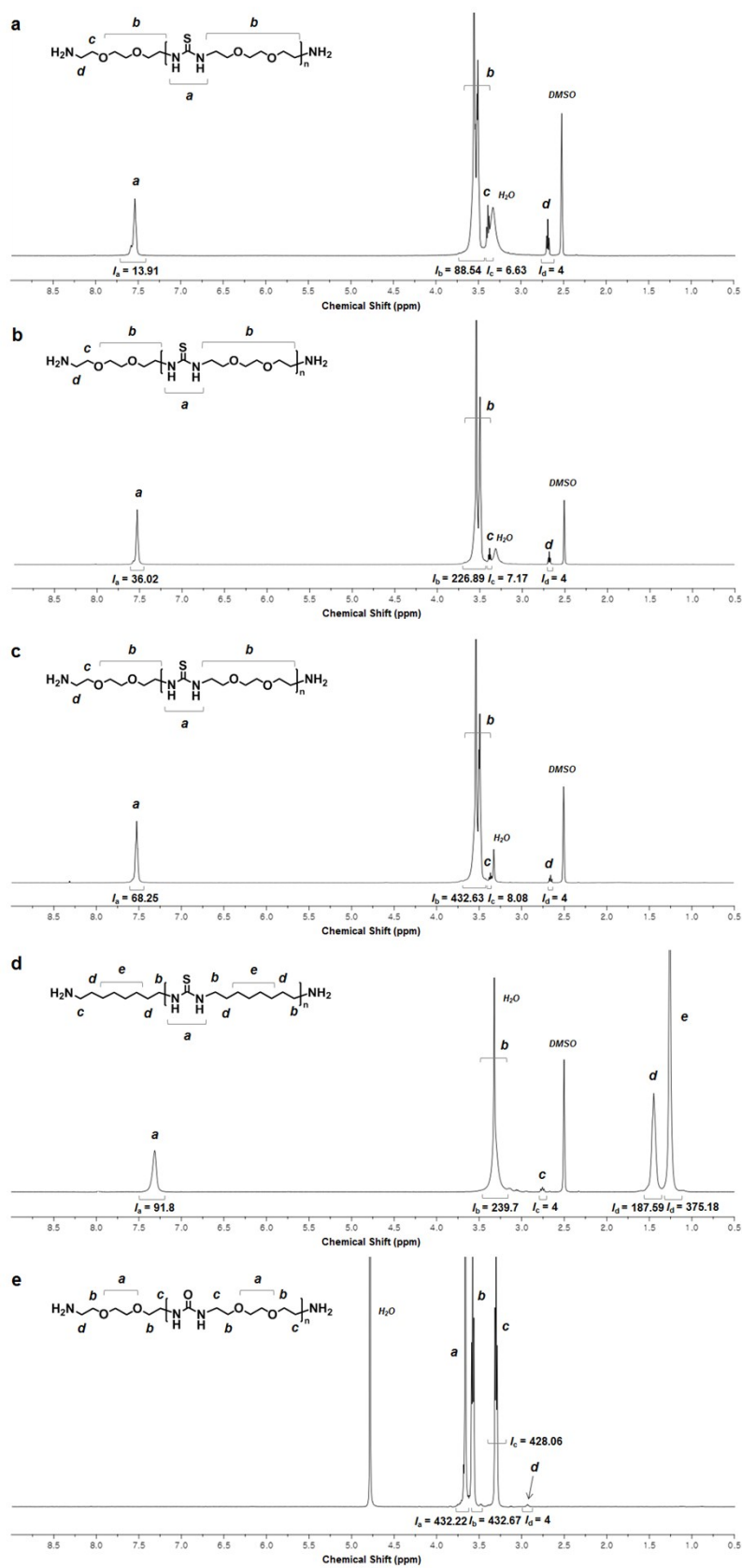
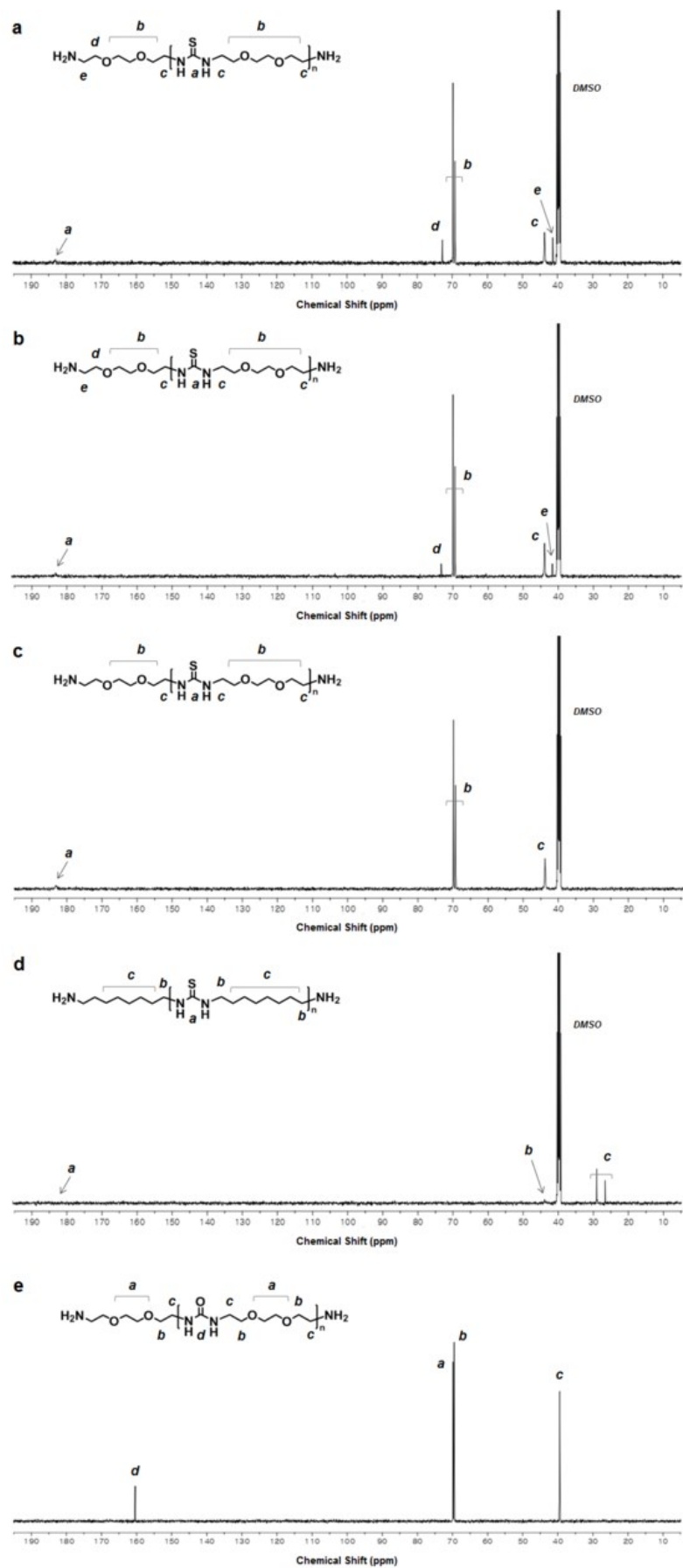**Fig. S2** ¹H NMR spectra of (a) TUEG7, (b) TUEG18, (c) TUEG34, (d) TUC46, and (e) UEG107.

Fig. S3 ¹³C NMR spectra of (a) TUEG7, (b) TUEG18, (c) TUEG34, (d) TUC46, and (e) UEG107.

Table S1 Characteristics of TUEGs, TUC, and UEG

Polymer	DP[a]	$M_{\text{n, NMR}}$[b] (g mol^{-1})	$M_{\text{n, GPC}}$ (g mol^{-1})	Đ
TUEG7	7	1,500	11,500[c]	1.31[c]
TUEG18	18	3,500	16,800[c]	1.30[c]
TUEG34	34	6,700	24,700[c]	1.48[c]
TUC46	46	8,700	19,800[c]	1.35[c]
UEG107	107	18,800	2,300[d]	4.03[d]

[a] Degree of polymerization, determined by ^{1}H NMR end group analysis. [b] Number-average molecular weight, calculated from $M_{\text{RU}} \times \text{DP} + M_{\text{EG}}$ (for TUEGs and UEG; or M_{OM} for TUC), where M_{RU}, M_{EG}, and M_{OM} are the molecular weights for repeating unit of polymer, 1,2-bis(2-aminoethoxy)ethane, and 1,8-diaminooctane, respectively. [c] Number-average molecular weight ($M_{\text{n, GPC}}$) and molecular weight dispersity (Đ), determined by GPC in DMF (with 0.01M LiBr) using a differential refractive index (RI) detector, calibrated with narrow-distribution polystyrene standards. [d] $M_{\text{n, GPC}}$ and Đ, determined by GPC in H$_2$O (pH = 7, with 0.2M NaNO$_3$ and 0.01M NaH$_2$PO$_4$) using a differential RI detector, calibrated with narrow-distribution polyethylene glycol standards.

The TUEGs and TUC46 possess polar thiourea functional groups, so that they dissolve well in polar solvents such as DMF, DMAc, and DMSO but do not dissolve in solvents of moderate polarity such as THF and CHCl$_3$. Thus, it is expected that the DMF used in GPC is a good solvent for the TUEGs and TUC. However, the DMF is a poor solvent for the calibration standard polystyrene without any polar functional groups,[S2] although the polystyrene is soluble in DMF and frequently used as a calibration standard for DMF GPC. This should result in smaller hydrodynamic volume of polystyrene in DMF, as compared with the polar TUEGs and TUC46. Therefore, the relative molecular weights of TUEGs and TUC46 in Table S1, characterized by the DMF GPC calibrated by polystyrene standards, are found to be much higher than the number-average molecular weights estimated by the ^{1}H NMR end group analysis. Meanwhile, the relative molecular weight of UEG107 was characterized by H$_2$O GPC calibrated with polyethylene glycol standards, due to its insolubility in DMF and DMAc. In comparison to the polyethylene glycol standards, the UEG107 possesses strong hydrogen bonding urea functional groups, which should lead to intramolecular hydrogen bonding interactions, thus resulting in smaller hydrodynamic volume in H$_2$O.[S3] Thus, the relative molecular weight of UEG107, characterized by the H$_2$O GPC calibrated with polyethylene glycol standards, is found to be much smaller than that characterized by ^{1}H NMR end group analysis.
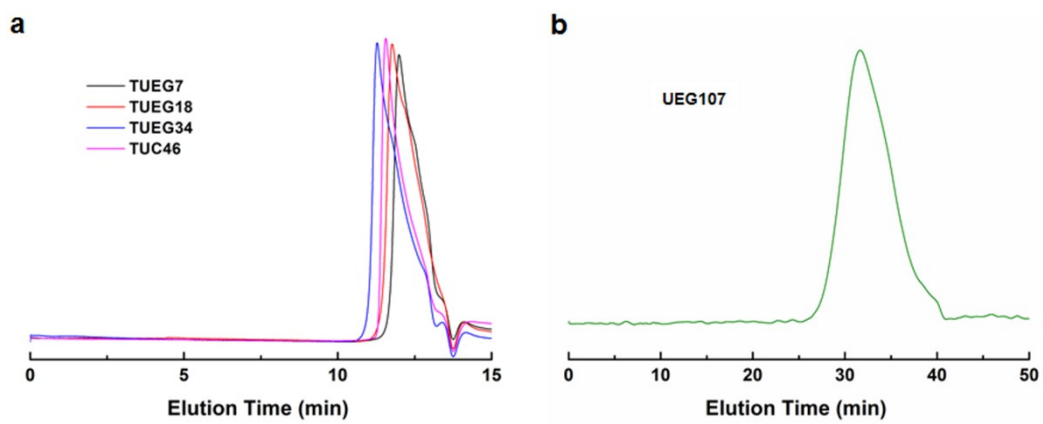
Fig. S4 GPC traces of (a) TUEGs and TUC46 in DMF and (b) UEG107 in H_2O.

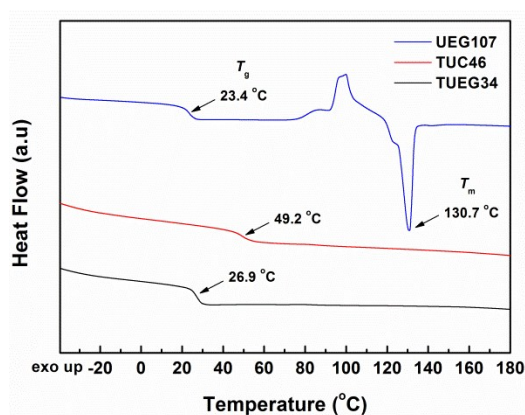## Thermal and Mechanical Characterization of TUEG34, TUC46, and UEG107

Fig. S5 DSC thermograms of TUEG34, TUC46, and UEG107 on the second heating (10 °C min⁻¹ for TUEG34 and TUC46, 5 °C min⁻¹ for UEG107).
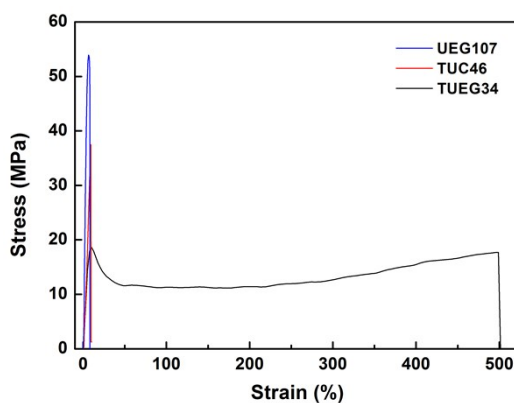

Fig. S6 Representative stress-strain curves of TUEG34, TUC46, and UEG107 at room temperature (26±1 °C) and a strain rate of 0.013 s⁻¹. TUEG34 exhibits somewhat lower elastic modulus/yield stress and higher extensibility, in comparison to the corresponding TUEG (measured at 21 °C) in the reference [S4]. This is mainly attributed to the higher experimental temperature in this study (26±1 °C), which is near the glass transition temperature of the TUEG. The TUEG34 exhibits much improved elastic modulus (1.2 Gpa) and yield stress (41 MPa) while slightly compromising extensibility (354%) at 21 °C; these values are similar to those of TUEG (measured at 21 °C) in the reference [S4].

Table S2 Summary of mechanical properties of TUEG34, TUC46, and UEG107 films

Sample	E^a (GPa)	σ_y^a (MPa)	ε_b^a (%)	U_T^a (MJ m^{-3})
TUEG34	0.7 ± 0.1	18 ± 1	500 ± 10	63 ± 3
TUC46	0.7 ± 0.2	41 ± 5	9 ± 2	2 ± 0
UEG107	1.5 ± 0.1	53 ± 2	10 ± 2	3 ± 1

[a] Determined from tensile testing at room temperature (26±1 °C) and a strain rate of 0.013 s^{-1}, where E, σ_y, ε_b, and U_T are elastic modulus, yield stress, strain at break, and toughness, respectively.
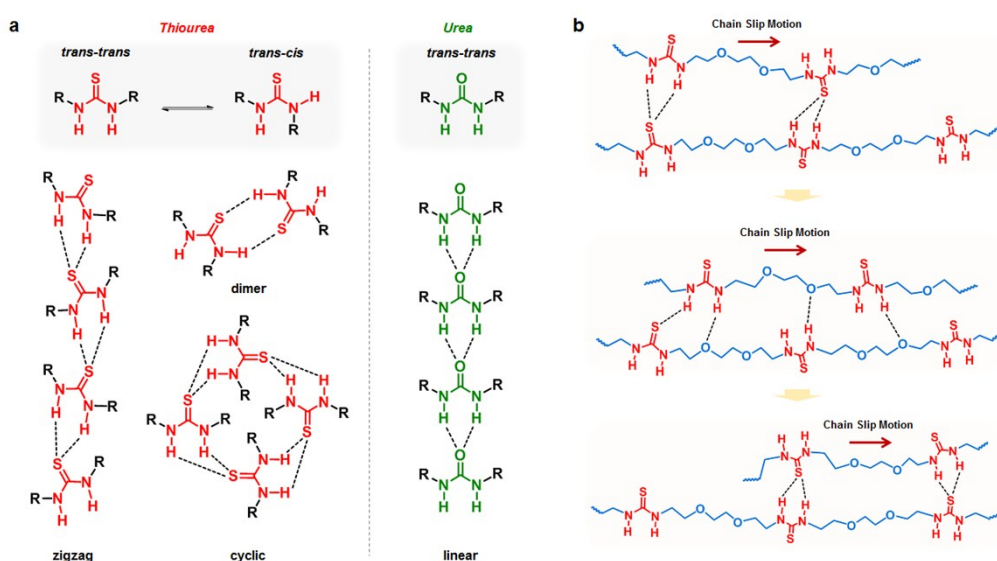
Fig. S7 Schematic illustrations of (a) different H-bonding interactions of thiourea and urea moieties in TUEG and UEG[S5] and (b) slip motions of TUEG polymer chains through facilitated H-bonding exchange with the aid of temporal H-bond acceptors in EG moieties.[S4]
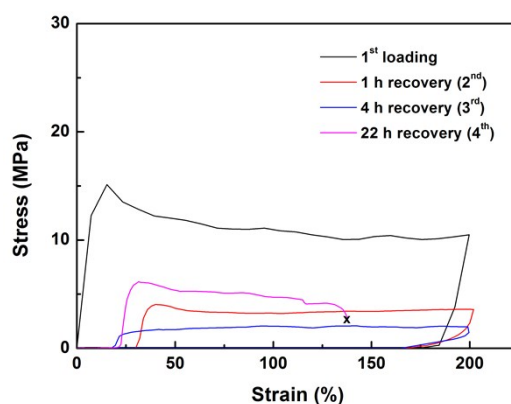
Fig. S8 Cyclic stress-strain curves of pristine TUEG34 (1st loading) and the pre-stretched TUEG34 after recovered for 1, 4, and 22 h at 25 °C. The cyclic tensile testing was performed at strain rate and limit of 0.0067 s^{-1} and 200%, respectively.
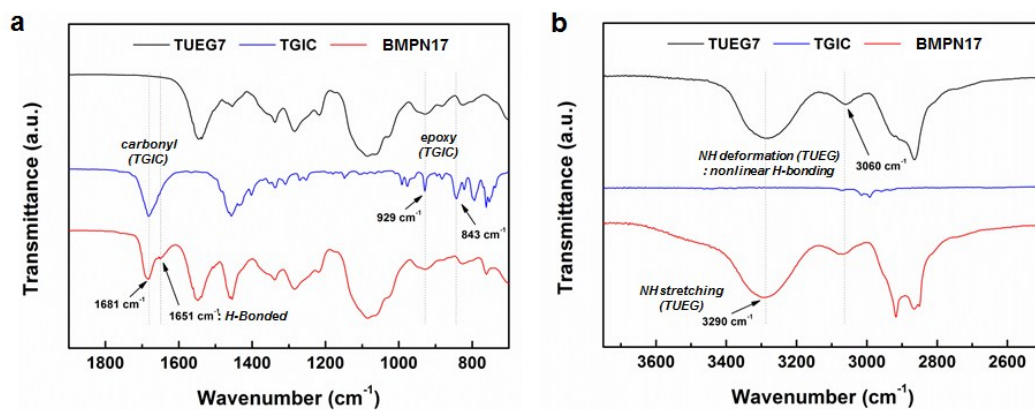
Preparation of BMPNs

Fig. S9 FT-IR spectra of TUEG7, TGIC, and BMPN17 in the wavenumber range of (a) 1900-700 cm⁻¹ and (b) 3750-2500 cm⁻¹.
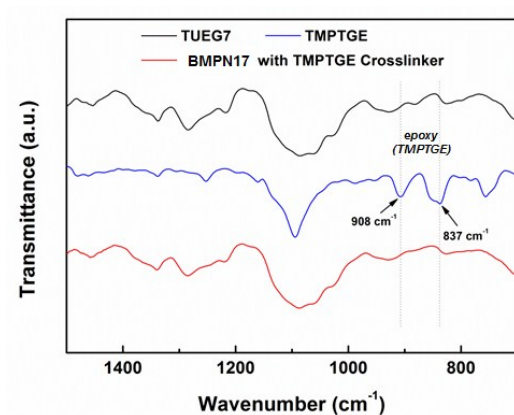

Fig. S10 FT-IR spectra of TUEG7, TMPTGE, and BMPN17 with TMPTGE crosslinker.
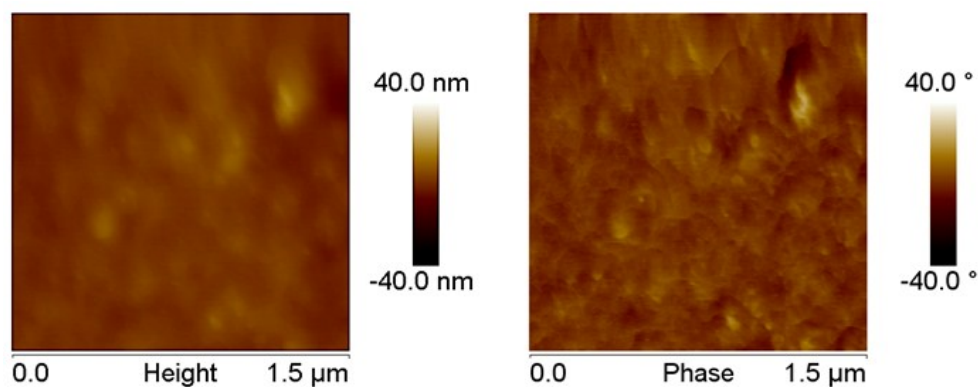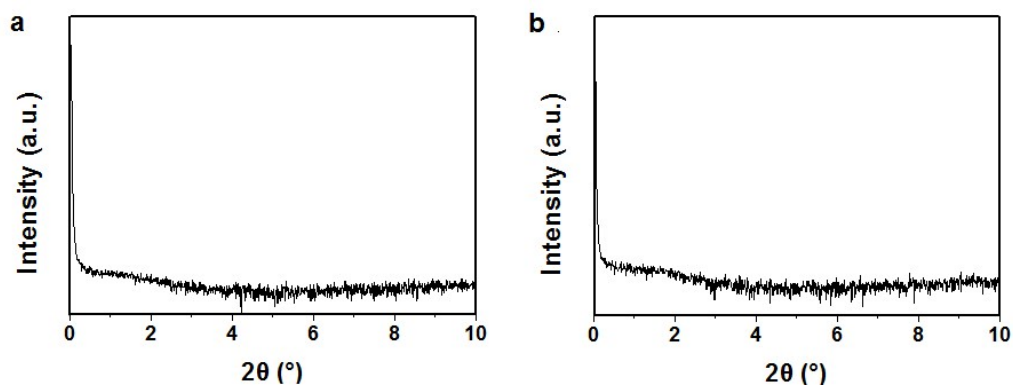

Fig. S11 AFM surface images of BMPN8.

Fig. S12 Small angle X-ray scattering (SAXS) profiles of (a) pristine and (b) 100% stretched BMPN8.
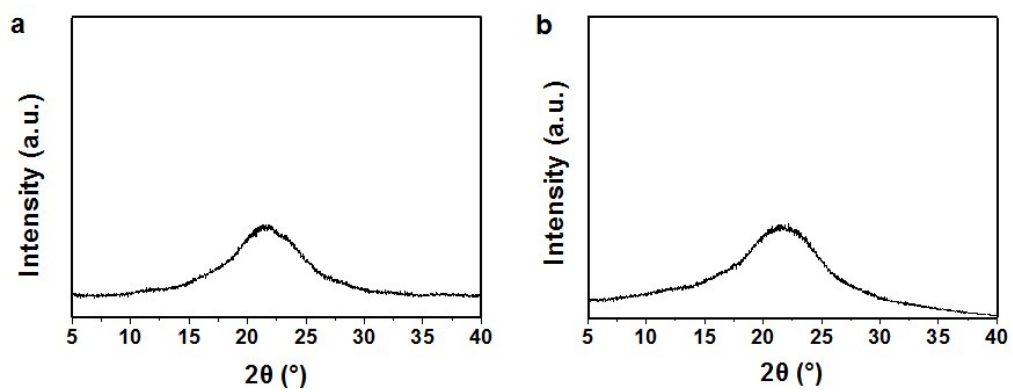

Fig. S13 Wide angle X-ray scattering (WAXS) profiles of (a) pristine and (b) 100% stretched BMPN8.
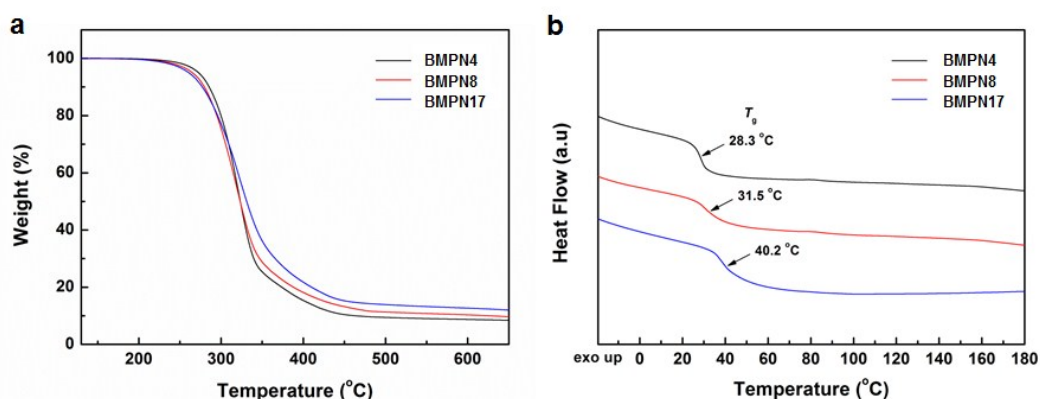
Thermal and Mechanical Characterization of BMPNs
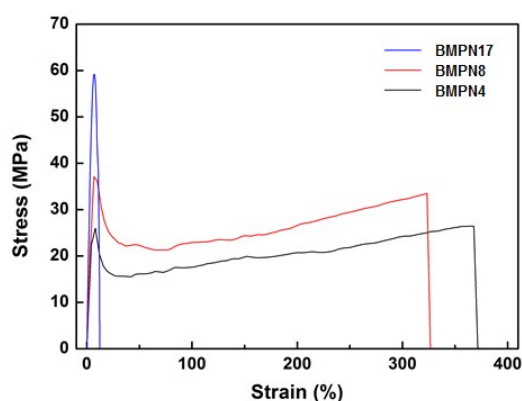

Fig. S14 (a) TGA curves and (b) DSC thermograms of BMPNs.

Fig. S15 Representative stress-strain curves of BMPNs at room temperature (26±1 °C) and a strain rate of 0.013 s⁻¹.

Table S3 Summary of thermal and mechanical properties of BMPN17 with TMPTGE cross-linker

Sample	$W_{TMPTGE}{}^{a}$	$f_g{}^{b}$	$T_g{}^{c}$ (°C)	E^{d} (GPa)	$\sigma_y{}^{d}$ (MPa)	$\varepsilon_b{}^{d}$ (%)	$U_T{}^{d}$ (MJ m⁻³)
BMPN17 with TMPTGE Crosslinker	0.17	0.90	35.2	1.0 ± 0.0	38 ± 4	220 ± 15	51 ± 6

[a] Weight fraction of TMPTGE in the sample. [b] Gel fraction, obtained by $f_g = W_a / W_d$, where W_d and W_a are the weights of dried film before and after N,N-dimethylformamide (DMF) solvent extraction. [c] Glass transition temperature, determined by DSC on the second heating at a rate of 10 °C min⁻¹. [d] Determined from tensile testing at room temperature (26±1 °C) and a strain rate of 0.013 s⁻¹, where E, σ_y, ε_b, and U_T are elastic modulus, yield stress, strain at break, and toughness, respectively.
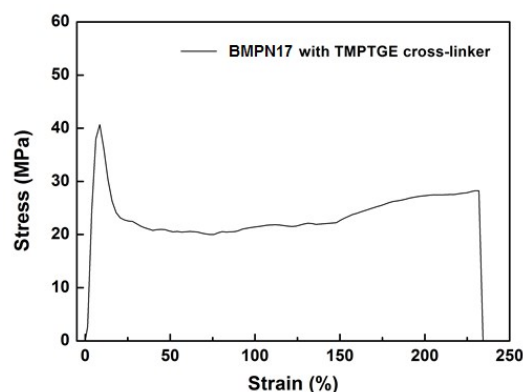
Fig. S16 Representative stress-strain curve of BMPN17 with TMPTGE cross-linker at room temperature (26±1 °C) and a strain rate of 0.013 s⁻¹.
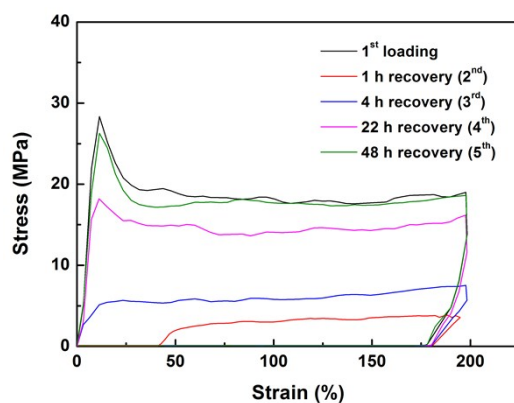

Fig. S17 Cyclic stress-strain curves of pristine BMPN4 (1st loading) and the pre-stretched BMPN4 after recovered for 1, 4, 22, and 48 h at 25 °C. The cyclic tensile testing was performed at strain rate and limit of 0.0067 s⁻¹ and 200%, respectively.
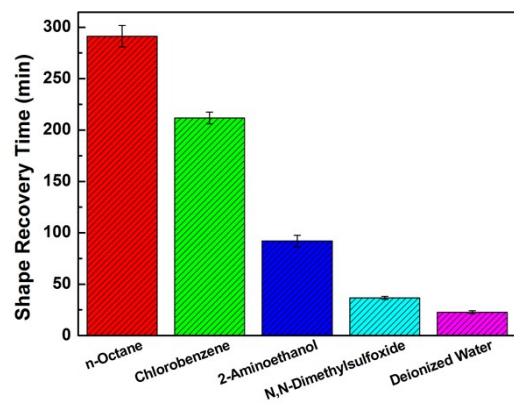

Fig. S18 Effect of different solvents on shape recovery times of temporarily shape-fixed BMPN8 film (ca. 18 mm (L) × 3 mm (W) × 0.35 mm (T)) at 25 °C.
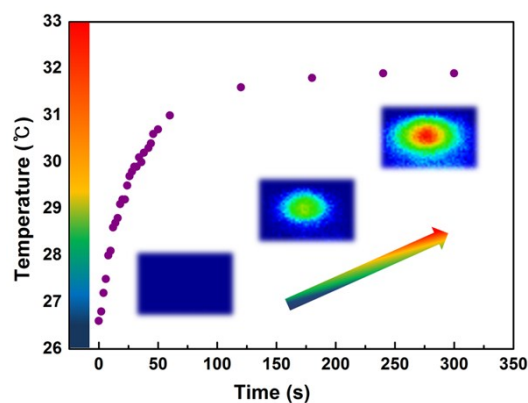
Fig. S19 Time-dependent temperature profile and IR images of BMPN8 upon 808 nm NIR laser irradiation (0.2 W mm^{-2}).
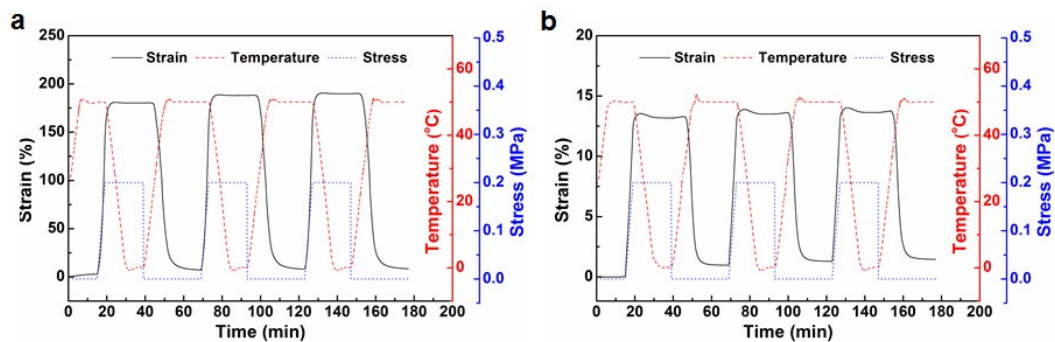

Fig. S20 Quantitative shape memory cycles of (a) BMPN4 and (b) BMPN17.

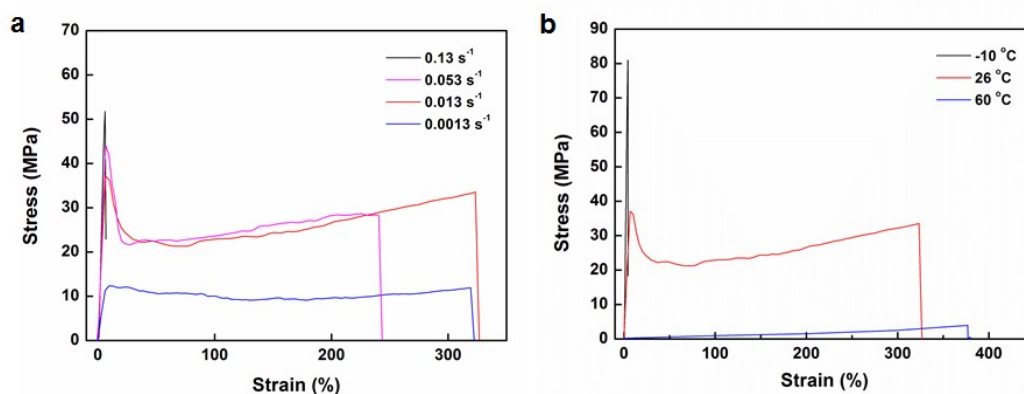**Fig. S21** Representative stress-strain curves of BMPN8 at (a) different strain rates (temperature = 26±1 °C) and (b) temperatures (strain rate = 0.013 s^{-1}).
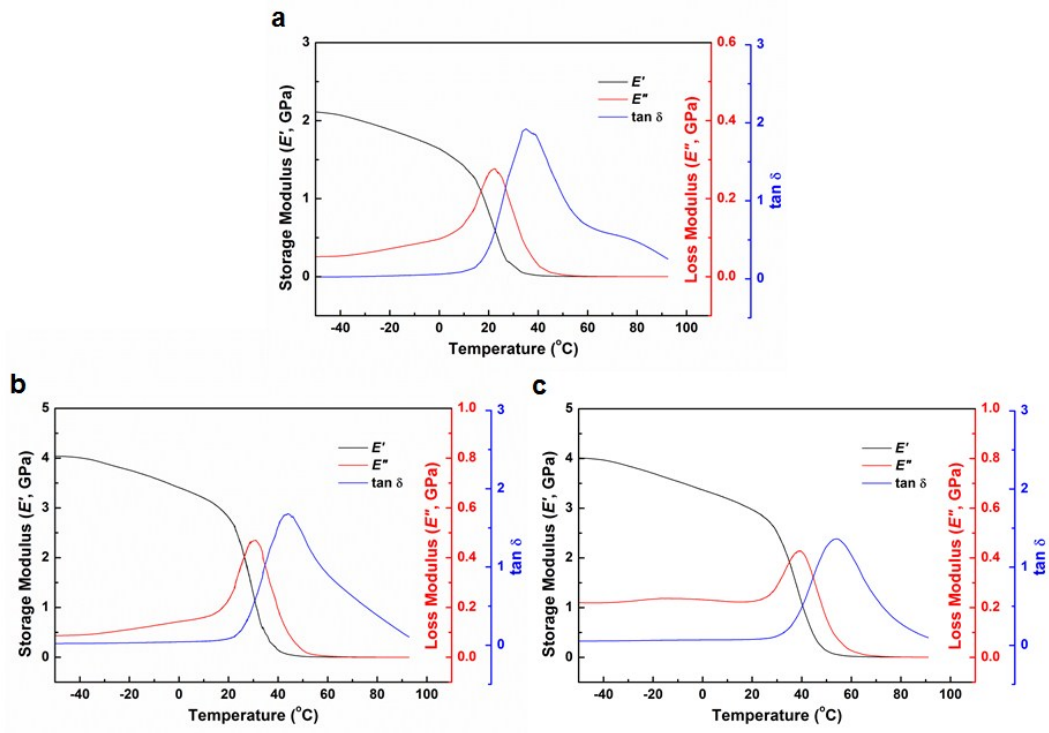
Fig. S22 DMA curves of (a) BMPN4, (b) BMPN8, and (c) BMPN17 at a constant frequency of 2.5 Hz and a heating rate of 5 °C min⁻¹.
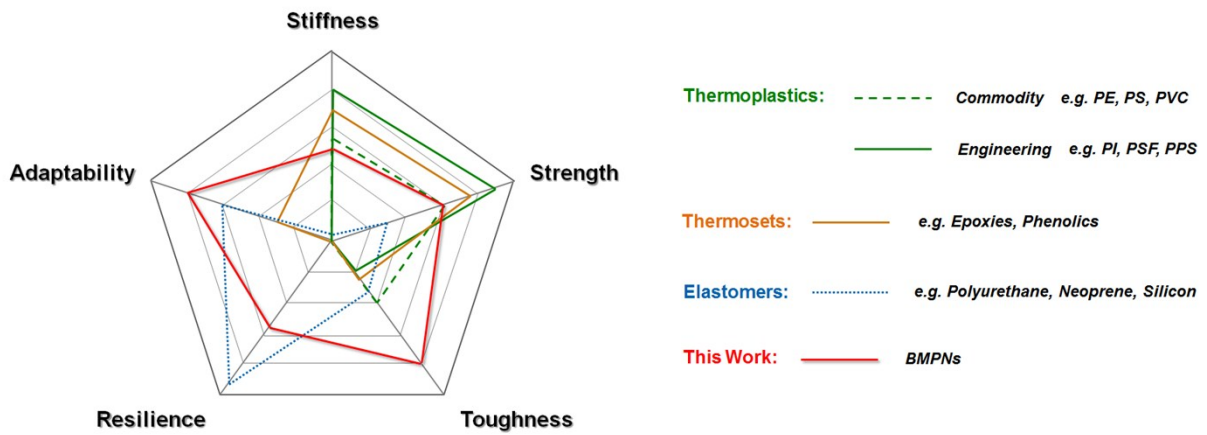

Fig. S23 Radar diagrams of versatile mechanical properties for BMPNs and conventional polymeric materials in the literature.[S6]

Table S4 Summary on mechanical properties of polymeric materials with noncovalent sacrificial bonds from recent literature reports

Type	System[a]	Noncovalent Interactions	Strain Rate (s⁻¹)	E^b (MPa)	σ_y^b (MPa)	σ_u^b (MPa)	ε_b^b (%)	Resilience[c]	Ref.
Hydrogel	CCN	Metal-ligand interactions	0.033	0.029	-	0.16	2,300	△	[S7]
	CCN	H-bonds	0.056	0.12	-	1	2,000	△	[S8]
	PCN	Ionic bonds	0.14	8	-	2	1,500	○	[S9]
	CCN	Dipole-dipole/ H-bonds	0.083	5.6	-	8.3	680	○	[S10]
	CCN	Metal-ligand interactions	0.042	17	-	10	330	○	[S11]
	PCN	Ionic bonds	0.14	7.9	-	5.1	750	○	[S12]
	PCN	H-bonds	0.017	0.15	-	0.95	1,200	○	[S13]
	CCN	H-bonds	0.1	28	2	2	800	○	[S14]
	CCN	H-bonds	0.001	2	-	2.7	81	○	[S15]
	CCN	Host-guest interactions	0.41	0.078	-	0.065	950	○	[S16]
Non-hydrated Polymer	PCN	H-bonds	0.006	200	5	10	100	○	[S17]
	CCN	H-bonds	0.11	2.3	-	1.7	940	○	[S18]
	PCN	H-bonds	0.007	13	-	0.92	320	○	[S19]
	PCN	Metal-ligand interactions	0.083	0.15	-	0.03	6,150	○	[S20]
	PCN	H-bonds	0.099	1.7	-	16	720	○	[S21]
	PCN	Metal-ligand interactions/ H-bonds	0.006	-	-	21	850	○	[S22]
	PCN	Metal-ligand interactions/ H-bonds	0.11	0.46	-	1.8	900	○	[S23]
	CCN	Metal-ligand interactions/ H-bonds	0.67	0.081	0.056	0.056	15,000	△	[S24]
	CCN	H-bonds	0.013	900	29	29	370	○	Present Study
	CCN	H-bonds	0.013	1,100	39	39	320	○	Present Study

[a] CCN = covalently cross-linked network, PCN = physically cross-linked network. [b] Determined from tensile testing, where E, σ_y, σ_u, and ε_b are elastic modulus, yield stress, ultimate tensile stress, and strain at break, respectively. [c] At room temperature. ○ = complete recovery of shape and mechanical properties after deformation, △ = partial recovery of shape and mechanical properties after deformation.

References for Electronic Supplementary Information

[S1]   (a) X. Wang and J. K. Gillham, *J. Appl. Polym. Sci.*, 1991, **43**, 2267.; (b) A. R. de Luzuriaga, R. Martin, N. Markaide, A. Rekondo, G. Cabañero, J. Rodríguez and I. Odriozola, *Mater. Horiz.* 2016, **3**, 241.

[S2]   J. V. Dawkins, *J. Polym. Sci., Polym. Phys. Ed.*, 1976, **14**, 569.

[S3]   P. J. M. Stals, M. A. J. Gillissen, R. Nicolaÿ, A. R. A. Palmans and E. W. Meijer, *Polym. Chem.*, 2013, **4**, 2584.

[S4]   Y. Yanagisawa, Y. Nan, K. Okuro and T. Aida, *Science*, 2018, **359**, 72.

[S5]   (a) R. Custelcean, M. G. Gorbunova and P. V. Bonnesen, *Chem. Eur. J.*, 2005, **11**, 1459; (b) R. Custelcean, *Chem. Commun.*, 2008, 295.

[S6]   (a) T. R. Crompton, *Physical Testing of Plastics*, Smithers Rapra, 2012, pp. 2-4; (b) Cambridge University Engineering Department, *Materials Data Book*, Cambridge, 2003, pp. 11-13.

[S7]   J.-Y. Sun, X. Zhao, W. R. K. Illeperuma, O. Chaudhuri, K. H. Oh, D. J. Mooney, J. J. Vlassak and Z. Suo, *Nature*, 2012, **489**, 133.

[S8]   Q. Chen, L. Zhu, C. Zhao, Q. Wang and J. Zheng, *Adv. Mater.*, 2013, **25**, 4171.

[S9]   T. L. Sun, T. Kurokawa, S. Kuroda, A. B. Ihsan, T. Akasaki, K. Sato, Md. A. Haque, T. Nakajima and J. P. Gong, *Nat. Mater.*, 2013, **12**, 932.

[S10]   Y. Zhang, Y. Li and W. Liu, *Adv. Funct. Mater.*, 2015, **25**,471.

[S11]   P. Lin, S. Ma, X. Wang and F. Zhou, *Adv. Mater.*, 2015, **27**, 2054.

[S12]   F. Luo, T. L. Sun, T. Nakajima, T. Kurokawa, Y. Zhao, K. Sato, A. B. Ihsan, X. Li, H. Guo and J. P. Gong, *Adv. Mater.*, 2015, **27**, 2722.

[S13]   X. Dai, Y. Zhang, L. Gao, T. Bai, W. Wang, Y. Cui and W. Liu, *Adv. Mater.*, 2015, **27**, 3566.

[S14]   X. Hu, M. Vatankhah-Varnoosfaderani, J. Zhou, Q. Li and S. S. Sheiko, *Adv. Mater.*, 2015, **27**, 6899.

[S15]   D. Zhao, J. Huang, Y. Zhong, K. Li, L. Zhang and J. Cai, *Adv. Funct. Mater.*, 2016, **26**, 6279.

[S16]   J. Liu, C. S. Y. Tan, Z. Yu, Y. Lan, C. Abell and O. A. Scherman, *Adv. Mater.*, 2017, **29**, 1604951.

[S17]   A. M. Kushner, J. D. Vossler, G. A. Williams and Z. Guan, *J. Am. Chem. Soc.*, 2009, **131**, 8766.

[S18]   J. A. Neal, D. Mozhdehi and Z. Guan, *J. Am. Chem. Soc.*, 2015, **137**, 4846.

[S19]   J-H Schuetz, P. Wentao and P. Vana, *Polym. Chem.*, 2015, **6**, 1714.

[S20]   C.-H. Li, C. Wang, C. Keplinger, J.-L. Zuo, L. Jin, Y. Sun, P. Zheng, Y. Cao, F. Lissel, C. Linder, X.-Z. You and Z. Bao, *Nat. Chem.*, 2016, **8**, 618.

[S21]   S. Yoshida, H. Ejima and N. Yoshie, *Adv. Funct. Mater.*, 2017, **27**, 1701670.

[S22]   J. Liu, J. Liu, S. Wang, J. Huang, S. Wu, Z. Tang, B. Guo and L. Zhang, *J. Mater. Chem. A*, 2017, **5**, 25660-25671.

[S23]   Q. Zhang, S. Niu, L. Wang, J. Lopez, S. Chen, Y. Cai, R. Du, Y. Liu, J.-C. Lai, L. Liu, C.-H. Li, X. Yan, C. Liu, J. B.-H. Tok, X. Jia and Z. Bao, *Adv. Mater.*, 2018, 1801435.

[S24]   Q. Zhang, C.-Y. Shi, D.-H. Qu, Y.-T. Long, B. L. Feringa and H. Tian, *Sci. Adv.*, 2018, **4**, eaat8192.